International Journal of Progressive Sciences and Technologies (IJPSAT)
ISSN: 2509-0119.

https://ijpsat.org/
Vol. 55 No. 2 February 2026, pp. 527-542

Prostate Cancer Proton Therapy Simulation Based On Homogeneous Water Equivalent Thickness Pencil Beam Model

Muhammad Fitriadi[1*], Heri Sutanto[2], Pandji Triadyaksa[3], Rizki Budiman[4]

[1]Student, Magister of Physics, Physics Department, Diponegoro University, Tembalang, Semarang, Indonesia
[2]Professor, Physics Department, Diponegoro University, Tembalang, Semarang, Indonesia
[3]Lecturer, Physics Department, Diponegoro University, Tembalang, Semarang, Indonesia
[4]Lecturer, Departemen of Physics, Matana University
*Corresponding Author: Pandji Triadyaksa. Email: triadyaksa@gmail.com

Abstract: Proton therapy is an important modality in the treatment of prostate cancer due to its ability to deliver precise doses to the target volume with minimal exposure to healthy tissue through the Bragg Peak characteristic. This study aims to develop a pencil beam simulation model integrated with homogeneous Water Equivalent Thickness (WET) using the Geant4 Monte Carlo simulation platform (version 11.2.1) to improve dose planning accuracy and efficiency. Simulations were conducted on a human phantom based on ICRP 145 with a detector resolution of 1 mm. The Spread-Out Bragg Peak (SOBP) was optimized at three irradiation angles (0°, 45°, 90°) using a Linear Least Squares (lsqlin) function to achieve a constant dose (Dconst) across the plateau region. Results showed a proton range uncertainty of <1 mm with optimal Dconst at angles 0°, 45°, and 90° of 0.66, 0.62, and 0.53 nGy/proton, respectively, covering depths of 7.32-10.21 cm, 9.68-12.48 cm, and 17.26-20.13 cm. The integration of homogeneous WET successfully simplified the computational burden while maintaining high accuracy, allowing it to be incorporated into conventional therapy planning systems. This model offers an efficient solution for facilities with limited capacity, although further clinical validation with real patient data is still required to ensure adaptability to individual anatomical variations.

Keywords: Bragg Peak, Prostate Cancer, Pencil Beam, Geant4 Simulation, Proton Therapy, Water Equivalent Thickness.

I. INTRODUCTION

Proton therapy is a significant innovation in cancer radiotherapy because it can reduce radiation exposure to healthy tissues through the Bragg Peak property, which stops energy precisely at the tumor location. Dose precision is achieved with the Spread-Out Bragg Peak (SOBP) configuration, which uses weighting factors for each proton beam to produce an even dose distribution throughout the tumor volume [1]. Prostate cancer, as one of the most commonly diagnosed cancers in men, has become a primary target for the development of this technology, given the high sensitivity of surrounding organs such as the rectum and bladder to radiation. Although the proportion of Proton Therapy use for prostate cancer decreased from 43.4% to 25% between 2012 and 2021, the number of cases continued to rise as the use of this therapy expanded to other types of cancer, including breast and head-and-neck cancers [2]. Globally, the number of Proton Therapy facilities has also continued to increase, with the emergence of smaller, more economically accessible centers, reaching more than 110 active facilities worldwide [3]. Nevertheless, significant challenges remain regarding dose planning accuracy, particularly due to reliance on Water Equivalent Thickness (WET) simulations in estimating proton range in heterogeneous tissues [3].

Several studies indicate that heterogeneity in WET values of immobilization devices can cause uncertainties in the proton range of around ±1 mm, which may risk disrupting the accuracy of radiation dose distribution [4]. Conventional pencil beam models

International Journal of Progressive Sciences and Technologies (IJPSAT)
ISSN: 2509-0119.

https://ijpsat.org/
Vol. 55 No. 2 February 2026, pp. 527-542

often do not account for this variability due to the assumption of material homogeneity, resulting in inaccurate predictions of the Bragg Peak depth [5]. Recent research through analysis of 15 clinical patients showed that the Treatment Planning System (TPS) underestimates the Stopping Power Ratio (SPR) of synthetic materials by an average of 20% (range: -35.1% to -0.2%), with dosimetric implications for organs at risk reaching up to 6.7% change in maximum dose [6]. In addition, the commonly used iterative numerical methods tend to be time-consuming and inefficient for routine clinical practice [6]. These imperfections increase the likelihood of underdosing tumor tissue or overdosing surrounding vital organs, which can ultimately reduce treatment success while increasing the potential for side effects [7].

This research aims to design a Proton Therapy simulation model for prostate cancer patients using a simple pencil beam approach from a synchrotron integrated with body materials assumed to be homogeneous water, with the primary goal of improving accuracy in dose planning while maintaining computational process efficiency. By conducting a quantitative analysis of the WET values of immobilization materials and prostate tissue, this study aims to provide a depiction of dose distribution in homogeneous water materials with less than 1 mm variation. Theoretically, this model has the potential to serve as a foundation for developing more flexible and clinically responsive therapy planning algorithms. Meanwhile, from a practical perspective, this approach offers a cost-efficient alternative, particularly for Proton Therapy facilities with limited resources. Therefore, this article is expected to make a tangible contribution to the improvement of clinical protocols and to expand access to precision radiation therapy for prostate cancer patients.

II. THEORETICAL FOUNDATION

2.1 Fundamental Principles of Proton Therapy in Radiation Oncology

Proton therapy is a charged particle radiotherapy modality that has undergone significant development since it was first proposed by Robert R. Wilson in 1946. The primary advantage of proton therapy lies in its unique energy deposition characteristics, fundamentally different from photons used in conventional radiotherapy. As protons traverse biological tissue, they lose energy gradually through Coulomb interactions with orbital electrons of atoms comprising the tissue. A remarkable phenomenon of this charged particle is that the greatest energy loss occurs at the end of its trajectory, just before the particle comes to a complete stop [8].

The fundamental difference between proton and conventional photon therapy lies in the dose distribution profile as a function of tissue depth. Photon beams experience maximum dose deposition at superficial depths, followed by exponential attenuation with increasing penetration depth. Consequently, healthy tissue traversed by the photon beam both anterior and posterior to the tumor target receives non negligible radiation dose. In contrast, protons exhibit a relatively low dose plateau in the initial portion of their trajectory, followed by a sharp increase in energy deposition at a specific depth that can be controlled through selection of the initial particle energy, with virtually no dose deposition in tissue beyond the target volume. This characteristic provides significant dosimetric advantage in protecting healthy tissue, particularly organs at risk (Organs at Risk, OAR) adjacent to the tumor [9].

2.2 Bragg Peak Phenomenon and Its Physical Mechanism

Bragg Peak is a physical phenomenon first observed by William Henry Bragg and his son William Lawrence Bragg in the early twentieth century during investigations of alpha particle interactions with matter. This phenomenon describes an extremely sharp peak in energy deposition at the terminus of a charged particle's trajectory when traversing a medium. This peak occurs because the cross section of ionization interactions increases as particle velocity decreases. Physically, the energy loss of a charged particle is inversely proportional to the square of its velocity, so when a proton slows near the end of its trajectory, the rate of energy loss per unit distance increases dramatically to a maximum just before the particle stops completely [8].

The energy deposition process of protons in biological tissue is dominated by electromagnetic interactions, specifically Coulomb interactions between protons and orbital electrons of target atoms. Each individual interaction produces atomic excitation or ionization, with relatively small energy transfer per event. However, the frequency of interactions increases significantly as

International Journal of Progressive Sciences and Technologies (IJPSAT)
ISSN: 2509-0119.

https://ijpsat.org/
Vol. 55 No. 2 February 2026, pp. 527-542

proton velocity decreases, causing accumulation of very large energy loss in the microscopic volume near the end of the proton trajectory. This produces the characteristic sharp and well-localized Bragg Peak [10], [11].

Quantitative description of proton energy loss in matter is provided by the Bethe-Bloch equation, which forms the theoretical foundation for understanding dose deposition in proton therapy. This equation describes the average rate of proton energy loss per unit trajectory length as a function of particle velocity, effective charge, and properties of the medium traversed. In its relativistic form, the Bethe Bloch equation shows that stopping power defined as $-dE/dx$ is inversely proportional to β^2, where β is the proton velocity relative to the speed of light. This means that the slower a proton moves, the greater the energy deposited per unit distance. This mathematically explains why Bragg Peak occurs at the end of the proton trajectory when velocity is lowest [8],[10].

For complex biological tissue, total stopping power is calculated using Bragg's rule (Bragg's rule), which states that the stopping power of a mixture is the weighted sum of the stopping powers of individual constituent elements based on their mass fractions. In the context of proton therapy planning, the concept of Stopping Power Ratio (SPR) becomes critically important. SPR is defined as the ratio of stopping power of a material to the stopping power of water at the same energy. Water is used as a reference standard because soft tissue composition is dominated by water, and dosimetric measurement is conveniently performed in water medium. Inaccurate SPR of tissue or immobilization devices can cause significant proton range uncertainty, with dosimetric implications reaching several percent at critical [6], [12].

2.3 Spread-Out Bragg Peak (SOBP) and Dose Distribution Optimization

The single Bragg Peak generated by a monoenergetic proton beam has an extremely narrow lateral width, typically only a few millimeters in the longitudinal direction. This characteristic becomes problematic in clinical application because the tumor volume requiring irradiation is generally far larger than the width of an individual Bragg Peak. If only a single proton energy is used, the majority of the tumor volume will not receive adequate radiation dose, while a small portion receives excessively high dose, resulting in highly inhomogeneous dose distribution [1].

To overcome this limitation, the concept of Spread-Out Bragg Peak (SOBP) was developed a superposition of multiple Bragg Peaks with different energies combined such that they produce a relatively flat and homogeneous dose plateau throughout the depth of the tumor volume. SOBP is created by combining proton beams with a varying energy spectrum, where each energy component contributes to dose deposition at specific depths. The highest energy beam reaches the deepest extent of the target volume, while progressively lower energy beams fill the more superficial layers [1].

The process of SOBP formation involves determining the intensity weighting factor (weighting factor) distribution for each proton energy component. These weighting factors must be designed such that the cumulative contribution from all energy components produces constant dose throughout the target depth. In this research, a numerical optimization approach based on Linear Least Squares (LLS) is employed to achieve optimal SOBP distribution. This method formulates the SOBP design problem as a constrained least squares minimization problem, where the objective is to minimize the squared deviation between actual dose distribution and desired target dose, with the constraint that all weighting factors must be non-negative [13], [14].

Mathematically, this problem is formulated by constructing a design matrix A of size $m \times n$ that stores dose profiles from n Bragg Peak components measured at m depth points within the target volume, vector b as the desired target dose vector (typically constant, Dconst, throughout the SOBP plateau), and vector w as the weighting factor vector to be optimized. The optimal solution w opt obtained from this optimization process is then used to construct the total dose profile as a weighted superposition. The LLS approach has advantages in computational efficiency and ability to accommodate additional clinical constraints, such as maximum dose limits at OAR or specific dose homogeneity requirements within the Planning Target Volume (PTV) [13], [15].

2.4 Pencil Beam Scanning and Intensity Modulated Proton Therapy

Pencil Beam Scanning (PBS) represents the most advanced and precise proton beam delivery technology in modern proton therapy. Unlike passive scattering techniques that use physical scatterers to widen the beam, PBS employs magnetic fields to

dynamically direct extremely narrow proton beams a few millimeters in diameter across the tumor volume in three dimensional patterns. The PBS system consists of a pair of scanning magnets (dipole magnets) capable of rapidly moving the proton beam in horizontal and vertical directions, enabling spot by spot dose delivery with high precision [16]. [17].

The primary advantage of PBS is its flexibility in creating three dimensional dose distributions highly conformal to complex and irregular tumor geometry. By controlling the lateral position of each proton spot through scanning magnets and regulating penetration depth through proton energy variation, the PBS system can "paint" dose with exceptional precision on each tumor layer. Each proton spot can be delivered with independently modulated intensity, providing complete three-dimensional dose distribution control. This technology enables superior dose conformality and optimal OAR protection compared to conventional passive scattering techniques [15]. [16].

Intensity Modulated Proton Therapy (IMPT) represents an advanced evolution of PBS that integrates intensity modulation techniques proven effective in Intensity Modulated Radiation Therapy (IMRT) with photons. In IMPT, the intensity of each proton spot is optimized independently through sophisticated planning algorithms to achieve complex dosimetric objectives, such as dose maximization to the PTV while minimizing dose to multiple OARs with different priorities. IMPT employs multiple beam angles and optimizes dose contribution from each direction simultaneously, enabling achievement of highly conformal dose distributions even for cases with extremely complex anatomy [16].

The IMPT optimization process involves solving a multi objective optimization problem with thousands to hundreds of thousands of variables intensities of individual proton spots and hundreds to thousands of dosimetric constraints specifying dose limits for various anatomical structures. The objective function typically employed is a weighted combination of various clinical criteria, such as dose deviation from prescription at the PTV, maximum and mean doses to OARs, and conformality and homogeneity factors. A significant advantage of IMPT is its capability to implement dose painting techniques, where different sub volumes within the tumor can receive different prescribed doses based on biological characteristics or histological aggressiveness [18], [19].

2.5 Water Equivalent Thickness (WET) in Proton Therapy Planning

Water Equivalent Thickness (WET) is a fundamental parameter in proton therapy planning that represents the equivalent water thickness producing the same stopping power as the actual proton trajectory through heterogeneous tissue or material. This concept is based on the fact that biological tissue composition is dominated by water approximately 70-80% of human body massand stopping power properties of most soft tissues are relatively similar to water. WET is defined as the integral of stopping power relative to water along the proton path. For homogeneous materials, WET can be simplified as the product of physical thickness and average SPR of the material [4], [17].

Accurate WET calculation is critically important in proton therapy because it determines proton range in tissue and consequently determines Bragg Peak location. Errors in WET estimation will cause longitudinal shift of dose distribution, potentially resulting in tumor underdosing if Bragg Peak falls anterior to the target, or overdosing of healthy tissue if Bragg Peak extends beyond the tumor's distal margin. WET uncertainty on the order of 1-2 mm can have significant clinical consequences, particularly for tumors adjacent to critical structures such as brainstem or optic nerve [4], [6].

In clinical practice, WET estimation is primarily based on conversion of Computed Tomography (CT) data using calibration curves that map Hounsfield Unit (HU) to SPR or mass density. These calibration curves are typically constructed by scanning tissue equivalent materials with known composition and density. However, several sources of uncertainty in this process can affect WET prediction accuracy. First, intrinsic CT imaging uncertainty, including noise, beam hardening artifacts, and scanner calibration variability, can cause fluctuation in HU values for the same tissue. Second, HU to SPR conversion involves assumptions regarding tissue elemental composition and mean excitation energy (I value), which can vary among individuals and differ from reference standard values. Third, immobilization device materials often possess significantly different composition from tissue equivalent materials used to create calibration curves, causing Treatment Planning System (TPS) to either underestimate or overestimate material SPR by as much as 20% or more [6], [12].

International Journal of Progressive Sciences and Technologies (IJPSAT)
ISSN: 2509-0119.

https://ijpsat.org/
Vol. 55 No. 2 February 2026, pp. 527-542

A comprehensive study by Jiang [6] demonstrated that TPS systematically underestimates SPR of immobilization devices commonly used in proton therapy by approximately 19.5% (range -35.1% to 0.2%). Although this SPR error is relatively large percentagewise, its dosimetric implication in most cases is minimal because absolute WET of immobilization devices is typically small due to material's low density, making absolute WET error usually less than 1-2 mm. However, for some critical OARs directly adjacent to the PTV, maximum dose changes up to 6.7% have been reported, indicating need for experimental SPR validation of immobilization devices during TPS commissioning. To reduce WET uncertainty, various strategies have been developed, including dual energy CT or spectral CT use for providing additional information on tissue elemental composition, direct SPR measurement using multilayer ionization chambers for immobilization devices, and implementation of robust optimization in therapy planning that explicitly accounts for range uncertainty [6], [12], [20].

2.6 Monte Carlo Simulation with Geant4 for Medical Physics Applications

Monte Carlo is a stochastic computational approach that simulates physical processes by tracking individual particle transport through a series of random interactions sampled from probability distributions consistent with underlying physical laws. In medical physics, particularly radiation therapy, Monte Carlo simulation permits highly accurate simulation of radiation dose deposition in complex geometries while accounting for all particle matter interaction processes, including multiple scattering, range straggling, and secondary particle production. Monte Carlo accuracy is based on the law of large numbers, which states that by simulating very large numbers of particles, the average simulation result will converge to the theoretical expected value of measured quantities. For radiation dosimetry, this means that simulated dose approaches actual dose with statistical uncertainty decreasing proportional to the square root of the number of particles simulated. Despite being computationally intensive, Monte Carlo is considered the gold standard for radiation dose calculation because of its ability to explicitly model particle transport physics without significant approximations [21], [22].

Geant4 (GEometry ANd Tracking) is an open source Monte Carlo simulation toolkit developed by an international collaboration for high energy physics and nuclear physics applications, but has been widely adopted in the medical physics community for dosimetry simulation, radiation therapy, and medical imaging. Geant4 is written in C++ with a highly modular and extensible object oriented architecture, permitting users to customize virtually every aspect of simulation for specific application needs. A primary advantage of Geant4 is its comprehensive physics models library, encompassing electromagnetic, hadronic, and optical processes for diverse particle types and broad energy ranges. For medical applications, Geant4 provides extensively validated physics lists, such as QGSP BIC HP recommended for proton therapy simulation. This physics list integrates accurate physics models for proton matter interactions, including ionization, excitation, multiple Coulomb scattering, and nuclear reactions, with accuracy verified through comparison to experimental data [11], [21].

Geant4 also provides highly flexible geometry modelling capabilities, permitting representation of complex geometries such as anthropomorphic phantoms with individually defined organs. For proton therapy applications, computational phantoms representing human anatomy realistically are essential for accurate therapy planning. ICRP Publication 145 provides Adult Mesh Type Reference Computational Phantoms (MRCPs) three dimensional representations of reference adult male and female anatomy, constructed from real human CT data and adjusted to ICRP reference anatomical parameters. MRCPs possess advantages over voxel phantoms in terms of deformability and scalability, permitting adaptation for varied body size and posture variations [23], [24].

In practice, Geant4 simulation for proton therapy involves several key components particle source definition (energy, position, direction), geometry construction (phantom, detectors), physics list selection, and output data collection (energy deposition, particle flux, spectrum). Detector scoring in Geant4 can be configured to measure various dosimetric quantities, such as dose per primary particle, depth dose distribution, or dose volume histogram for specific anatomical structures. With detector segmentation at high spatial resolution such as 1 mm as employed in this research dose profiles with high precision can be obtained for analysis of Bragg Peak characteristics and SOBP verification [11], [21].

International Journal of Progressive Sciences and Technologies (IJPSAT)
ISSN: 2509-0119.

https://ijpsat.org/
Vol. 55 No. 2 February 2026, pp. 527-542

2.7 Prostate Cancer as a Target for Proton Therapy

Prostate cancer is one of the most frequently diagnosed malignancies in men worldwide, with incidence continuing to increase with aging populations and improved early detection methods. Although the majority of prostate cancer cases are indolent and manageable with active surveillance, a significant proportion of patients require definitive therapy including radical surgery, external beam radiotherapy, or brachytherapy. External beam radiotherapy has become one of the primary modalities for localized prostate cancer with local control and survival rates comparable to radical prostatectomy [25].

The primary challenge in prostate cancer radiotherapy is the anatomical proximity of the prostate to organs highly radiosensitive, particularly the rectum, bladder, and penile bulb. The rectum, located directly posterior to the prostate, is highly vulnerable to radiation exposure causing acute and chronic gastrointestinal toxicity, including proctitis, rectal bleeding, and in severe cases, rectovesical fistula. The bladder, adjacent to the anterior and superior prostate aspects, also risks developing toxicity including cystitis, hematuria, and incontinence. Preservation of sexual and urinary function is an important treatment planning priority, given the significant impact of therapy toxicity on patient quality of life [25].

Proton therapy offers significant dosimetric advantages for prostate cancer compared to conventional photon radiotherapy or even IMRT. Bragg Peak characteristics enable selective high dose deposition to the prostate volume while minimizing dose to rectum and bladder. Lateral or anterior oblique beam configurations can be optimized to position Bragg Peak distal fall-off beyond the prostate's posterior margin, such that the rectum posterior to the prostate receives minimal dose compared to photon techniques where exit dose is unavoidable [26].

Comparative dosimetric studies have demonstrated that proton therapy can reduce integral dose to healthy tissue by 50% or more compared to photon IMRT for prostate cancer cases. Significant reductions in rectal volume receiving moderate to high doses (V40-V70) have been consistently reported, with potential implications for decreased risk of grade 2-3 rectal toxicity, one of the most bothersome side effects of prostate radiotherapy. Similarly, bladder dose, particularly to the trigone and bladder neck which are most sensitive, can be substantially reduced through optimal beam angle selection [13], [26].

Although the dosimetric benefits of proton therapy are clear, optimal clinical implementation requires special attention to technical aspects unique to protons. Range uncertainty is a critical issue that must be addressed through robust planning strategies, where the treatment plan is optimized to maintain dosimetric objectives even in worst case range error scenarios. For prostate cancer, range uncertainty is particularly relevant in the anterior posterior direction where protons traverse tissue of varying density such as abdominal wall, periprostatic fat, and bladder with changing fill level. Use of homogeneous WET as an approximation can simplify calculation and enhance computational efficiency, but validation against more complex models and clinical data remains necessary to ensure therapy safety and effectiveness [13], [26].

III. RESEARCH METHODOLOGY

The research flow begins with a literature review to formulate the basis for proton therapy simulation for prostate cancer, including understanding Water Equivalent Thickness (WET) and the formation of the Spread-Out Bragg Peak (SOBP). The first implementation stage involves calculating the WET of the prostate and surrounding areas to estimate the range of the prostate, which determines the selection of Bragg Peak energy and depth.

The next step is to build the SOBP profile through multi-energy files, creating a homogeneous dose plateau within the Planning Target Volume (PTV). Dose simulation is performed on a representative anatomical model while adhering to Organ at Risk (OAR) tolerance limits, resulting in a dose distribution. The discussion includes verification of range, dose homogeneity, and compliance with OAR limits, providing a solid basis for drawing research conclusions. The research flow diagram can be seen in Figure 1.

International Journal of Progressive Sciences and Technologies (IJPSAT)
ISSN: 2509-0119.

https://ijpsat.org/
Vol. 55 No. 2 February 2026, pp. 527-542

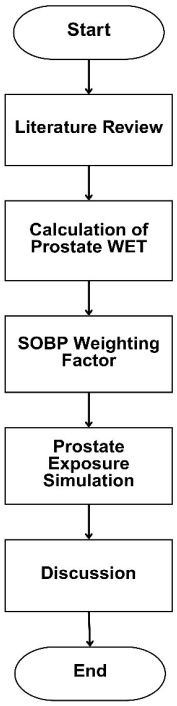

Figure 1: Research flow diagram

3.1 Literacy study

This study uses Monte Carlo simulation with Geant4 software version 11.2.1 [21] to calculate the proton therapy dose distribution for prostate cancer using an MRCPs phantom model based on ICRP 145 data. The simulation was run on the Linux Mint 21.3 "Virginia" operating system with hardware specifications of an AMD Ryzen 5 5600 processor and 32 GB DDR4 RAM. The physics list serves to define the physical processes that will be executed during the simulation. The physics list used is QGSP_BIC_HP, which is recommended for medical applications. The proton source is modeled as a pencil beam using the Geant4 Monte Carlo simulation [24].

3.2 *Water Equivalent Thickness* (WET)

Water Equivalent Thickness (WET) represents the thickness of a tissue path equated to water along the proton beam path. This value is calculated from the body surface to the target (prostate), with the beam isocenter as the reference point. WET is obtained from the effective length of the proton path to the prostate, making it easier to adjust the range or reach and beam energy in therapy planning, where the WET value is approximated for body tissue materials that have density and mass stopping power similar to water (homogeneous) [27].

To reduce high doses to the rectum, reference is taken from [26], which compares two techniques: Bilateral (BL) irradiation from the lateral direction and Anterior Oblique (AO) irradiation from the anterior oblique direction. Technically, an anterior beam design with an angle of about ±35°, as shown in Figure 2, is used as a representative configuration. This approach provides optimal dose coverage to the prostate while reducing exposure to rectal organs at risk (OAR).

International Journal of Progressive Sciences and Technologies (IJPSAT)
ISSN: 2509-0119.

https://ijpsat.org/
Vol. 55 No. 2 February 2026, pp. 527-542

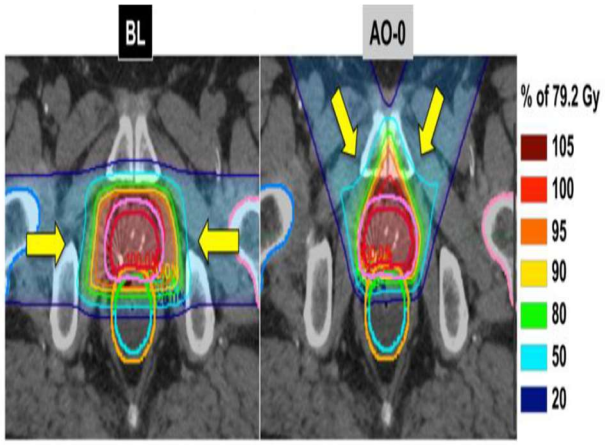

Figure 2: Proton beams for a. Bilateral (BL) and b. Anterior Oblique (AO) [27].

This WET study will calculate the angles of proton beams fired at the prostate: 0° (Anterior) Direction toward the front of the prostate, near the bladder neck and proximal urethra; 45° (Right Anterolateral) Direction diagonal between the anterior and right lateral; 90° (Right Lateral) Direction toward the right side of the prostate, away from the midline. The geometry shape is shown in Figure 3.

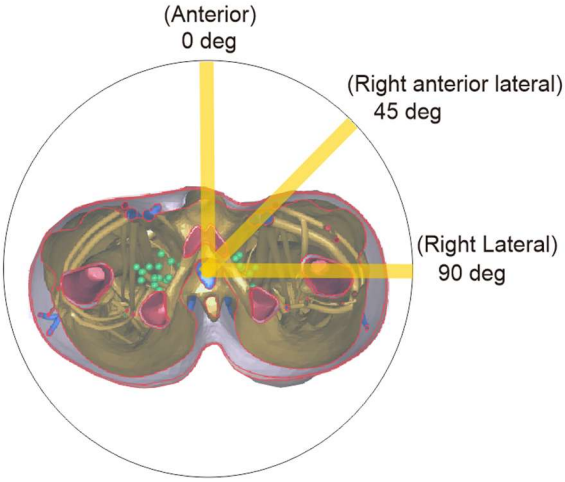

Figure 3: Transversal section view of the prostate with irradiation directions at 0°, 45°, and 90°.

3.3 Spread-Out Bragg Peak (SOBP) Simulation

A 100 mm × 100 mm × 300 mm water phantom simulation is used as the test basis, with a detector segmented at 1 mm in the depth direction to obtain high-resolution dose distribution, as shown in Figure 2. Each proton is assumed to have a parallel path with no scattering angle. The proton beam weighting factor, calculated by MATLAB Linear Least Squares (lsqlin), is a numerical vector where each element represents the relative contribution of each proton energy to the total dose distribution in the Spread-Out Bragg Peak (SOBP) configuration. This vector is generated through an optimization process that minimizes the difference between the desired dose (Dconst) and the actual dose. Dconst is the constant dose value along the plateau, also called the flat region of the SOBP, aimed at ensuring a uniform dose throughout the target volume.

International Journal of Progressive Sciences and Technologies (IJPSAT)
ISSN: 2509-0119.

https://ijpsat.org/
Vol. 55 No. 2 February 2026, pp. 527-542

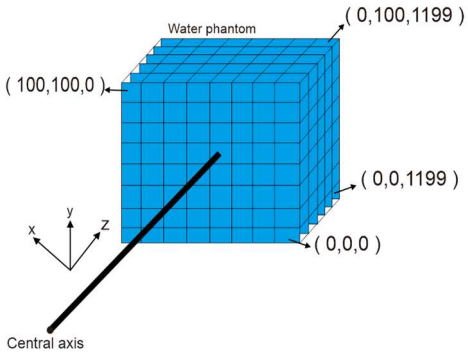

Figure 4: Illustration of the water phantom and detector segmentation index.

The central axis dose distribution is calculated from proton energy data in 1 MeV increments. Protons are absorbed by the detector segments and converted from MeV to nGy/proton using a Python script on Google Colab. The spot scanning beam configuration is carried out at 3 irradiation angles (0°, 45°, and 90°) to create a uniform dose profile (Spread Out Bragg Peak/SOBP) according to the Water Equivalent Thickness (WET) of the prostate, which is calculated based on the irradiation angles.

To achieve a uniform dose distribution in the SOBP (Spread-Out Bragg Peak) plateau region in proton therapy, we applied optimization of Bragg Peak (BP) component weights using the lsqlin function (Linear Least Squares constrained optimization) in MATLAB. The design matrix A (m×n) is constructed based on the dose profiles of n BP components measured at m depth points in the target area, while the target vector **b** defined as *D*const. The optimization process is carried out to minimize the squared residuals $|\mathbf{Aw}-\mathbf{b}|^2$ with constraints $\mathbf{w} \geq 0$ so that the obtained weight is always non-negative, where $\mathbf{w}_{opt}$ is the optimized weight vector [13]. Optimal weight $\mathbf{w}_{opt}$ which is used to compile the total dose profile $D_{tot}(z) = \sum_{i=1}^{f} wiDi(z)$ which approaches Dconst on the plateau. In this equation,$D_{tot}(z)$ represents the magnitude of the dose at depth$z$. Value wi is a weighting factor for high-energy pencil beams i, sedangkan $Di(z)$ depict the dose distribution at depth z produced by the pencil beam. The variable i indicates the pencil beam index, while f represents the total number of pencil beams used. This formulation allows the combination of several pencil beams with different energies to produce a uniform dose profile in the target area [15].

3.4 Prostate exposure simulation

In this simulation, the design of the configuration and the shape of the Spread Out Bragg Peak (SOBP) distribution was carried out, optimized to deliver a uniform dose throughout the prostate volume. The design process began with an approximation using a water phantom, followed by the calculation of the dose received by each organ using the ICRP 145 phantom model [23]. Dose coverage of the prostate volume was estimated through an analysis of the Water Equivalent Thickness (WET) of the prostate for each irradiation direction. The SOBP design was constructed based on proton beam segments that contributed dose at specific depths, then refined through optimization using the lsqlin method to obtain the most effective configuration. This resulting configuration was subsequently used in a proton beam irradiation simulation on a water phantom to evaluate the resulting dose distribution and to ensure that the irradiation target across the entire prostate area was optimally achieved.

IV. RESULTS AND DISCUSSION

This study successfully developed a proton therapy simulation model for prostate cancer using a pencil beam approach integrated with homogeneous Water Equivalent Thickness (WET) values through the Geant4 Monte Carlo simulation platform, as shown in Table 1.

International Journal of Progressive Sciences and Technologies (IJPSAT)
ISSN: 2509-0119.

https://ijpsat.org/
Vol. 55 No. 2 February 2026, pp. 527-542

Table 1 Distribution of proton energy weight in each direction in the prostate

Length	2,9 cm	2,8 cm	2,9 cm
Direction	0 deg	45 deg	90 deg
Depth	7,32 to 10,21 cm	9,68 to 12,48 cm	17,26 to 20,13 cm
Dconst	0,66	0,62	0,53
Energy	weight	weight	weight
82.3 MeV	0	0	0
84.0 MeV	0	0	0
85.8 MeV	0	0	0
87.6 MeV	0	0	0
89.3 MeV	0	0	0
91.1 MeV	0	0	0
92.8 MeV	0	0	0
94.6 MeV	0	0	0
96.3 MeV	0,0189	0	0
98.1 MeV	0,0281	0	0
99.8 MeV	0,0301	0	0
101.6 MeV	0,0322	0	0
103.3 MeV	0,0353	0	0
105.1 MeV	0,0386	0	0
106.8 MeV	0,0434	0	0
108.6 MeV	0,0475	0	0
110.3 MeV	0,0558	0	0
112.1 MeV	0,0637	0	0
113.8 MeV	0,0786	0,0293	0
115.6 MeV	0,1018	0,0319	0
117.4 MeV	0,1995	0,0352	0
119.2 MeV	0,2265	0,0367	0
120.9 MeV	0	0,0406	0
122.7 MeV	0	0,0448	0
124.4 MeV	0	0,0512	0
Length	2,9 cm	2,8 cm	2,9 cm
Direction	0 deg	45 deg	90 deg
Depth	7,32 to 10,21 cm	9,68 to 12,48 cm	17,26 to 20,13 cm
Dconst	0,66	0,62	0,53
Energy	weight	weight	weight
126.2 MeV	0	0,0579	0
127.9 MeV	0	0,0684	0
129.7 MeV	0	0,0852	0
131.4 MeV	0	0,1088	0
133.2 MeV	0	0,2505	0
134.9 MeV	0	0,1594	0
136.7 MeV	0	0	0
138.4 MeV	0	0	0
140.2 MeV	0	0	0
141.9 MeV	0	0	0
143.6 MeV	0	0	0
145.4 MeV	0	0	0
147.1 MeV	0	0	0
148.9 MeV	0	0	0
150.6 MeV	0	0	0
152.4 MeV	0	0	0
154.1 MeV	0	0	0

International Journal of Progressive Sciences and Technologies (IJPSAT)
ISSN: 2509-0119.

https://ijpsat.org/
Vol. 55 No. 2 February 2026, pp. 527-542

155.9 MeV	0	0	0
157.6 MeV	0	0	0,0361
159.4 MeV	0	0	0,0400
161.2 MeV	0	0	0,0404
162.9 MeV	0	0	0,0495
164.7 MeV	0	0	0,0526
166.4 MeV	0	0	0,0642
168.2 MeV	0	0	0,0794
170.0 MeV	0	0	0,1090
171.7 MeV	0	0	0,1086
173.4 MeV	0	0	0,4201

Table 1 shows the distribution of optimized proton energy weights for three irradiation angles (0 deg, 45 deg, 90 deg) in prostate cancer therapy. At 0 deg (anterior), the effective energy range is 96.3-119.2 MeV with a maximum weight of 0.2265 at 119.2 MeV, targeting a prostate depth of 7.32-10.21 cm. For the 45 deg (anterolateral) angle, higher energies (113.8-134.9 MeV) are used with a peak weight of 0.2505 at 133.2 MeV, reaching depths of 9.68-12.48 cm. Meanwhile, the 90 deg (lateral) angle requires the highest energies (157.6-173.4 MeV) with a dominant weight of 0.4201 at 173.4 MeV for penetration depths of 17.26-20.13 cm.

Table 1 presents the graph results of the study, which show that at a 0 degree angle, protons reach a depth of 7.32-10.21 cm with a concentrated dose (Dconst) of 0.66, as seen in Figure 3, while at 45 degrees and 90 degrees, they show deeper penetration of 9.68-12.48 cm (Dconst 0.62) and 17.26-20.13 cm (Dconst 0.53), respectively, which can be seen in Figures 3 and 4.

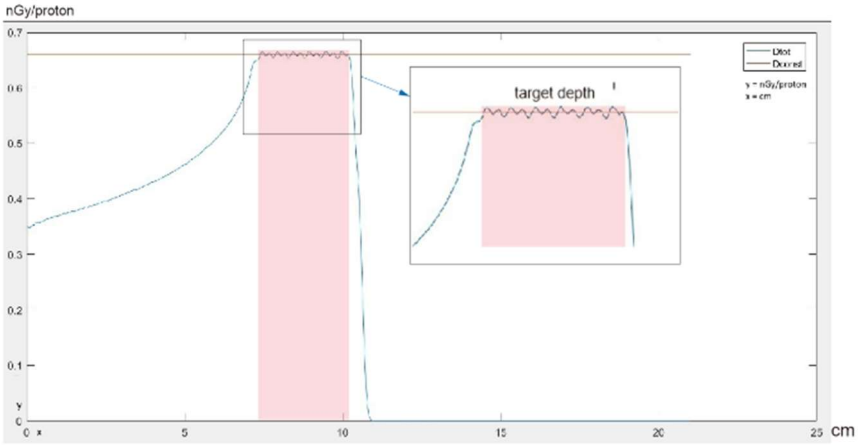

Figure 5: graph of absorbed dose per proton particle versus prostate depth at 0 deg angle, Dconst 0.66

International Journal of Progressive Sciences and Technologies (IJPSAT)
ISSN: 2509-0119.

https://ijpsat.org/
Vol. 55 No. 2 February 2026, pp. 527-542

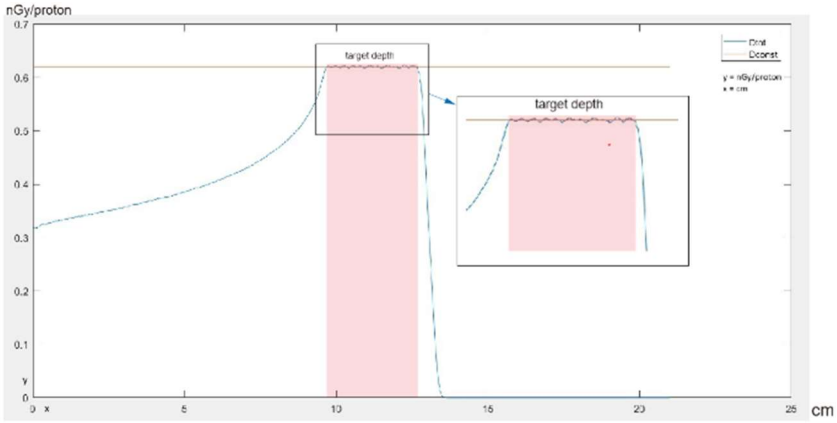

Figure 6: graph of absorbed dose per proton particle versus prostate depth at 45 deg angle, Dconst 0.62

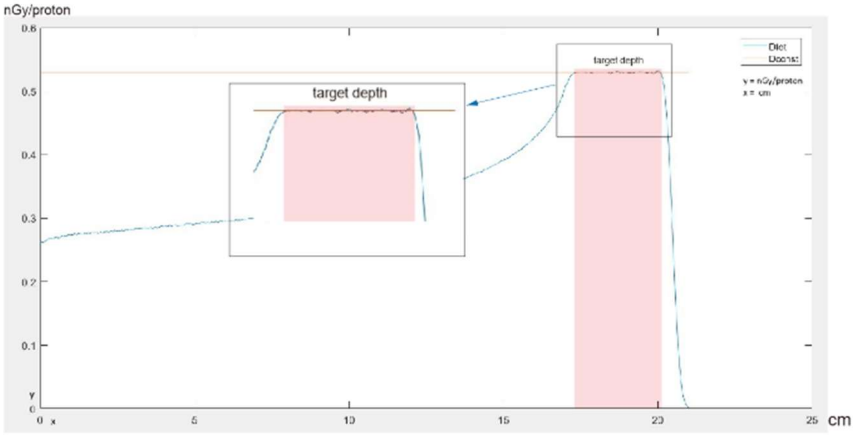

Figure 7: graph of absorbed dose per proton particle versus prostate depth at 90 deg angle, Dconst 0.53

Simulations show a significant influence of the irradiation angle on the depth of the Bragg Peak and Dconst. At angles of 0 deg, 45 deg, and 90 deg, Dconst are 0.66, 0.62, and 0.53, respectively, as seen in Table 2. The decrease in Dconst values with increasing angle is caused by the longer proton path or mass stopping power, as illustrated in Figures 8-10, which show the variation of dose profiles based on the irradiation angle.

Table 2 Simulation Results of Proton Dose Distribution in the Prostate.

Prostate length	Direction	Initial and final depth	Dconst
2,9 cm	0 deg	7,32 - 10,21 cm	0,66
2,8 cm	45 deg	9,68 - 12,48 cm	0,62
2,9 cm	90 deg	17,26 - 20,13 cm	0,53

International Journal of Progressive Sciences and Technologies (IJPSAT)
ISSN: 2509-0119.

https://ijpsat.org/
Vol. 55 No. 2 February 2026, pp. 527-542

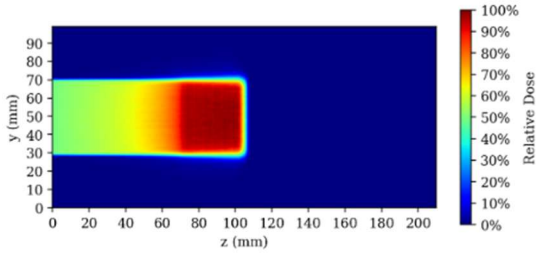

Figure 8: Dose distribution profile of proton therapy beam fired at 0 degrees

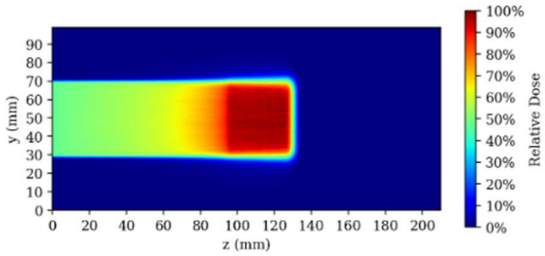

Figure 9: Dose distribution profile of proton therapy beam fired at 45 degrees

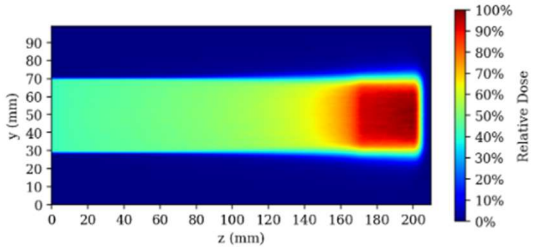

Figure 10: Dose distribution profile of proton therapy beam fired at 90 degrees

This study developed a proton therapy simulation model for prostate cancer by integrating homogeneous Water Equivalent Thickness (WET) into a pencil beam approach based on the Monte Carlo Geant4 simulation platform version 11.2.1. The main findings indicate that the proton irradiation angles (0°, 45°, and 90°) significantly affect the Bragg Peak penetration depth and the constant dose value (Dconst). At a 0° angle (anterior), the Bragg Peak depth reaches 7.32-10.21 cm with a Dconst of 0.66 nGy/proton, while the 45° (anterolateral) and 90° (lateral) angles reach depths of 9.68-12.48 cm (Dconst 0.62) and 17.26-20.13 cm (Dconst 0.53), respectively. This pattern follows the principle of proton physics where energy increases with target depth [9], with greater weight given to high energy to compensate for flux reduction at depth [17]. The integration of homogeneous WET in the pencil beam model successfully simplified computational calculations without compromising proton range accuracy, with uncertainties of less than 1 mm. The combination of 45° and 90° irradiation angles in this study aligns with recent findings showing that pencil beam scanning with angle optimization results in improved therapeutic outcomes for prostate cancer, with a multi-angle approach proven superior to single-angle techniques. This offers a potentially more favorable clinical outcome in reducing doses to organs at risk (OAR) such as the rectum, compared to single-angle 0° irradiation.

Quantitative data in Table 1, Table 2, and the dose profile visuals in Figures 8-10 show a consistent and complementary relationship. At a 0° angle (Figure 8), the effective proton energy ranges from 96.3 to 119.2 MeV with a maximum weight of 0.2265 at 119.2 MeV, resulting in a stable dose plateau corresponding to a Dconst of 0.66 nGy/proton, with an energy range of 113.8-134.9 MeV and a peak weight of 0.2505 at 133.2 MeV, yielding a Dconst of 0.62 nGy/proton. At a 90° angle, higher energies (157.6-173.4 MeV) are required with a maximum weight of 0.4201 at 173.4 MeV to achieve the deepest penetration, each resulting in a Dconst of 0.53 nGy/proton. The consistency between theoretical predictions and simulation results validates the model's accuracy,

particularly in predicting the Bragg peak depth and the energy weight distribution at various irradiation angles. The use of a water phantom with a 1 mm resolution detector allows for precise dose measurement, especially in determining the location and characteristics of the Bragg Peak. The proton range uncertainty of less than 1 mm indicates that the developed homogeneous WET model has a high level of reliability in predicting proton penetration in prostate tissue [28].

Dosimetric analysis shows that the irradiation angle significantly affects the dose distribution characteristics and proton penetration. The decrease in the Dconst value with increasing irradiation angle (from 0.66 at 0° to 0.53 at 90°) can be explained by the law of mass stopping power. At 0° (anterior), protons travel the shortest path to the prostate, which is located in front at a distance of approximately 7.32–10.21 cm. At 45° (anterolateral), the travel distance increases to 9.68–12.48 cm, and at 90° (lateral), protons must penetrate deeper, up to 17.26–20.13 cm to reach the prostate volume.

According to the Bethe Bloch law, the energy of protons gradually decreases as the travel distance within the medium increases. The longer the path that must be traversed, the more energy is lost through ionization interactions [8]. This phenomenon is reflected in Table 1, where a 90° angle requires much higher proton energy (up to 173.4 MeV) compared to a 0° angle (maximum 119.2 MeV) to reach the prostate volume at the same depth. The dosimetric consequence is that the Dconst value at a 90° angle (0.53 nGy/proton) is lower compared to that at a 0° angle (0.66 nGy/proton).

From a clinical perspective, the combination of 45° and 90° beam angles shows advantages in reducing radiation exposure to organs at risk (OAR), particularly the rectum and sigmoid colon. The sharper distal fall-off at the 90° angle (as shown in Figure 10) provides better protection for the tissue behind the prostate. Additionally, the three-beam geometry (0°, 45°, 90°) allows for a more even distribution of dose across the prostate volume, reducing hot spots (high-dose areas) and cold spots (low-dose areas), thereby improving dose uniformity in the target and lowering the risk of complications in OARs. The use of a water phantom with 1 mm resolution detectors enables precise dose measurements, particularly in determining the location of the Bragg Peak. However, it should be noted that the assumption of parallel proton paths without scattering may not fully reflect the complexity of real clinical conditions [13].

The integration of homogeneous WET values into the pencil beam model successfully simplifies calculations without compromising accuracy, with proton range uncertainty of less than 1 mm. This approach addresses the limitations of conventional models, which often overlook variations in immobilization material density. The computational efficiency of this model is demonstrated by its ability to generate a Spread Out Bragg Peak (SOBP) with three irradiation angles in a relatively short time. From a clinical perspective, this model offers an economical and effective solution for healthcare facilities with limited resources. However, this study still has limitations, as it has not yet considered dynamic factors such as organ movement or inter-patient anatomical variations, and the use of static water phantoms does not fully represent the heterogeneity of prostate tissue.

V. CONCLUSION

Based on the research results, it can be concluded that the Geant4-based simulation model with homogeneous WET integration and the pencil beam approach successfully achieved high dose distribution accuracy, with proton range uncertainty of less than 1 mm. The proton irradiation angle was found to have a significant influence on penetration depth and dose profile, with Dconst values ranging from 0.53 to 0.66 depending on the angle. These findings have important implications, as the Dconst value in proton therapy simulation planning optimization ensures that the entire tumor volume receives a uniform dose while avoiding underdosing or overdosing, thereby effectively protecting healthy tissues.

REFERENCES

[1]. D. Jette and W. Chen, "Creating a spread-out Bragg peak in proton beams" Physics in Medicine and Biology, 56(11), (2011). doi:10.1088/0031-9155/56/11/N01.

[2]. Hartsell WF, Simone CB 2nd, Godes D, Maggiore J, Mehta MP, Frank SJ, Metz JM, Choi JI. Temporal Evolution and Diagnostic Diversification of Patients Receiving Proton Therapy in the United States: A Ten-Year Trend Analysis (2012 to

2021) From the National Association for Proton Therapy. Int J Radiat Oncol Biol Phys. 2024 Jul 15;119(4):1069-1077. doi: 10.1016/j.ijrobp.2023.12.041.

[3]. Wroe AJ, Ghebremedhin A, Gordon IR, Schulte RW, Slater JD. Water equivalent thickness analysis of immobilization devices for clinical implementation in proton therapy. Technol Cancer Res Treat. 2014 Oct;13(5):415-20. doi: 10.7785/tcrtexpress.2013.600260.

[4]. Zhang R, Newhauser WD. Calculation of water equivalent thickness of materials of arbitrary density, elemental composition and thickness in proton beam irradiation. Phys Med Biol. 2009 Mar 21;54(6):1383-95. doi: 10.1088/0031-9155/54/6/001.

[5]. ScienceDirect. A Model for Secondary Monitor Unit Calculations of PBS Terapi Proton. Radiother Oncol. 2023;145:88-95. doi:10.1016/j.radonc.2023.02.015.

[6]. Jiang K, MacFarlane M, Mossahebi S, Zakhary MJ. Evaluation of treatment planning system accuracy in estimating the stopping-power ratio of immobilization devices for proton therapy. J Appl Clin Med Phys. 2023 Feb;24(2):e13831.doi:10.1002/acm2.13831.

[7]. Zahra Hashemi, Mansoureh Tatari, Haladhara Naik, Simulation of dose distribution and secondary particle production in proton therapy of brain tumor, Reports of Practical Oncology & Radiotherapy, Volume 25, Issue 6, 2020, Pages 927-933, ISSN 1507-1367,https://doi.org/10.1016/j.rpor.2020.08.015.

[8]. Martinez, D. M., Rahmani, M., Burbadge, C., Lee, S. H., Cascio, E. W., Papiez, L., Moskvin, V., & Timmerman, R. (2019). A practical solution of the Bethe equation in the energy range applicable to radiotherapy and radionuclide production. Scientific Reports, 9, Article 17599. https://doi.org/10.1038/s41598-019-54103-3.

[9]. Paganetti, H. (2012). Range uncertainties in proton therapy and the role of Monte Carlo simulations. Physics in Medicine & Biology, 57(11), R99–R117. https://doi.org/10.1088/0031-9155/57/11/R99.

[10]. Mohammed, M. I. (2024). Theoretical study of energy loss of proton in human tissues. Ibn AL-Haitham Journal For Pure and Applied Sciences, 37(4), 162–171. https://doi.org/10.30526/37.4.3245.

[11]. Arce, P., Bolst, D., Bordage, M. C., Brown, J. M. C., Cirrone, P., Cortés-Giraldo, M. A., Cutajar, D., Cuttone, G., Desorgher, L., Dondero, P., Dusseau, L., Faddegon, B., Fancher, C., Guatelli, S., Incerti, S., Ivanchenko, V., Jacquet, M., Karamitros, M., Kyriakou, I., Villagrasa, C. (2021). Report on G4-Med, a Geant4 benchmarking system for medical physics applications developed by the Geant4 Medical Simulation Benchmarking Group. Medical Physics, 48(1), 19–56. https://doi.org/10.1002/mp.14226.

[12]. Peters, N., Wohlfahrt, P., Hofmann, C., Möhler, C., Menkel, S., Tschiche, M., Krause, M., Troost, E. G. C., Richter, C., & Jakobi, A. (2023). Consensus guide on CT-based prediction of stopping-power ratio using a Hounsfield look-up table for proton therapy. Radiotherapy and Oncology, 184, Article 109675. https://doi.org/10.1016/j.radonc.2023.109675.

[13]. Unkelbach J, et al. Optimization of intensity modulated proton therapy. Med Phys. 2009;36(5):1813-1821. doi:10.1118/1.3110081.

[14]. Chen, Y., Michalski, D., Houser, C., & Galvin, J. M. (2002). A deterministic iterative least-squares algorithm for beam weight optimization in conformal radiotherapy. Physics in Medicine & Biology, 47(10), 1647–1658. https://doi.org/10.1088/0031-9155/47/10/303.

[15]. Budiman R, Sutanto H, Tursinah R, Triadyaksa P. Dose distribution of pencil beam proton therapy using Geant4 simulation for breast cancer treatment. J Phys Its Appl. 2025;7(2):48-53. doi:10.14710/jpa.2025.48-53.

[16]. Chang, J. Y., Zhang, X., Knopf, A., Li, H., Mori, S., Dong, L., Lu, H. M., Liu, Q., Liao, Z., Hobbs, B., Shen, J., Jeter, M., Gomez, D. R., Welsh, J. W., Gillin, M. T., Hocht, S., Flampouri, S., Lin, S. H., Li, Z., Mohan, R. (2017). Consensus guidelines for implementing pencil-beam scanning proton therapy for thoracic malignancies on behalf of the PTCOG thoracic and

lymphoma subcommittee. International Journal of Radiation Oncology, Biology, Physics, 99(1), 41–50. https://doi.org/10.1016/j.ijrobp.2017.05.014.

[17]. Lomax, A. J., Boehringer, T., Coray, A., Egger, E., Goitein, G., Grossmann, M., Juelke, P., Lin, S., Pedroni, E., Rohrer, B., Roser, W., Rossi, B., Siegenthaler, B., Stadelmann, O., Stauble, H., Vetter, C., & Wisser, L. (2020). Treatment planning for proton therapy: What is needed in the next 10 years? British Journal of Radiology, 93(1107), Article 20190359. https://doi.org/10.1259/bjr.20190359.

[18]. Schaub, S. K., Hartvigson, P. E., Lock, M. I., Høyer, M., Brunner, T. B., Cardenes, H. R., Dawson, L. A., Kim, E., Klages, P., Parikh, P. J., Rwigema, J. C. M., Seong, J., Willett, C., Mendez Romero, A., Goodman, K. A., & Haddock, M. G. (2020). Intensity-modulated proton therapy using dose-painting pencil beam scanning for high-risk hepatocellular carcinoma. Journal of Clinical Oncology, 38(4_suppl), Article 558. https://doi.org/10.1200/JCO.2020.38.4_suppl.558.

[19]. Vítek, P., Doležel, M., Vaculíková, M., Bělohlávek, P., & Boháčová, P. (2021). Pencil beam scanning (PBS) intensity modulated proton therapy (IMPT) for anal cancer. Radiation Oncology, 16, Article 253. https://doi.org/10.1186/s13014-021-01979-9.

[20]. Inaniwa, T., Suzuki, M., Sato, S., Noda, A., Iwata, Y., Kanematsu, N., & Kohno, R. (2023). Stopping-power ratio of body tissues with updated effective energies and I-values. Medical Physics, 50(6), 3488–3496. https://doi.org/10.1002/mp.16324.

[21]. Agostinelli, S., Allison, J., Amako, K., Apostolakis, J., Araujo, H., Arce, P., Asai, M., Axen, D., Banerjee, S., Barrand, G., Behner, F., Bellagamba, L., Boudreau, J., Broglia, L., Brunengo, A., Burkhardt, H., Chauvie, S., Chuma, J., Chytracek, R., ... Zschiesche, D. (2003). Geant4 a simulation toolkit. Nuclear Instruments and Methods in Physics Research Section A: Accelerators, Spectrometers, Detectors and Associated Equipment, 506(3), 250–303. https://doi.org/10.1016/S0168-9002(03)01368-8.

[22]. Kochebina, O., Bär, E., Battistoni, G., Boehlen, T., Boswell, C., Chandra, R., Chiriotti, S., Cirrone, G. A. P., Cuttone, G., Guatelli, S., Höss, M., Janeiro, L., Lestand, L., Lund, E., Muraro, S., Patera, V., Perl, J., Resch, A., Romano, F., ... Grevillot, L. (2024). GATE Monte Carlo simulation toolkit for medical physics. EPJ Web of Conferences, 295, Article 04043. https://doi.org/10.1051/epjconf/202429504043.

[23]. International Commission on Radiological Protection (ICRP). (2020). Adult reference computational phantoms. ICRP Publication 145. Annals of the ICRP, 49(1), 1–125. https://doi.org/10.1177/0146645320911864.

[24]. Kim, C. H., Yeom, Y. S., Nguyen, T. T., Han, M. C., Choi, C., Lee, H., Shin, B., Griffin, K. T., Bolch, W. E., & Lee, C. (2020). ICRP Publication 145: Adult mesh-type reference computational phantoms. Annals of the ICRP, 49(3), 13–201. https://doi.org/10.1177/0146645319893605.

[25]. Biegała, M., Kopeć, M., & Dąbrowski, T. (2016). Analysis of dose distribution in organs at risk in patients with prostate cancer treated with ionizing radiation. Reports of Practical Oncology & Radiotherapy, 21(5), 428–436. https://doi.org/10.1016/j.rpor.2016.04.004.

[26]. Moteabbed, M., Trofimov, A., & Paganetti, H. (2017). Optimization of beam angles for proton therapy of prostate cancer. Medical Physics, 44(6), 2512–2521. https://doi.org/10.1002/mp.12255.

[27]. Schneider U, et al. Calculation of water equivalent thickness of materials of arbitrary density. Med Phys. 2009;36(7):3108-3121. doi:10.1118/1.3148582.

[28]. Gottschalk B, et al. Water equivalent path length calibration for proton therapy. Phys Med Biol. 2015;60(17):6675-6693. doi:10.1088/0031-9155/60/17/6675.

Click or tap here to enter text.